

## Electron capture by and electron excitation of two-electron fluorine ions incident on helium

M. Terasawa,\* Tom J. Gray, S. Haggmann, J. Hall, J. Newcomb,  
P. Pepmiller, and Patrick Richard

*Department of Physics, Kansas State University, Manhattan, Kansas 66506*

(Received 6 July 1981; revised manuscript received 20 December 1982)

It is demonstrated that the total F *K* x-ray production cross section for  $F^{7+} + He$  collisions comes predominantly from three types of processes. These processes are 1s-electron excitation of the  $1s^2\ ^1S$  ground state of  $F^{7+}$ , 2s electron excitation of the  $1s2s\ ^3S$  metastable state of  $F^{7+}$ , and *nl* electron capture by the  $1s2s\ ^3S$  metastable state of  $F^{7+}$ . All three of these processes have one thing in common, namely, they result in F *K* x rays. By using a high-resolution x-ray spectrometer, the cross sections for the three processes are measured separately as a function of projectile energy in the range of 6 to 40 MeV. The assignment of the three different processes of 1s electron excitation, 2s electron excitation, and *nl* electron capture is corroborated by comparing the measured energy dependences of the various *K* x-ray transitions with theory and other experimental measurements with  $F^{8+}$  and  $F^{9+}$  beams.

### I. INTRODUCTION

Atomic collisions of fluorine ions incident on helium have been investigated recently by high-resolution x-ray measurements which allow one to distinguish collision processes to various final states in the projectile ion.<sup>1-4</sup> A number of x-ray transitions originate from the decay of initial states produced by electron excitation of, ionization of, or electron capture by the fluorine ions. It was shown that the excitation process and the ionization process are strongly dependent on the electron configuration of the incident F ions and that the excitation cross section is larger than the ionization cross section for the higher charge states of the F ions.<sup>3</sup>

Recent studies include the incident energy dependence of x-ray production in  $F^{9+}$ ,  $F^{8+}$ , and  $F^{6+}$ -He collisions up to about 40 MeV.<sup>2,4</sup> The studies showed that the electron-excitation process is dominant over electron capture at high incident energies in  $F^{8+}$ -He collisions. In the  $F^{6+}$ -He collisions, electron excitation dominates over all other *K*-shell processes for the energy range up to 40 MeV. The *K*-vacancy production processes in  $F^{6+} + He$  collisions can occur via two two-step processes. These two-step processes are 2s electron ionization plus 1s-2p excitation and 1s electron ionization plus 2s-2p excitation.<sup>4</sup>

For two-electron-bearing  $F^{7+}$  ions, there is an experimental difficulty in obtaining pure  $1s^2\ F^{7+}$  beams. It is well known that a moderate fraction of the two-electron ion beam is composed of the long-lived  $1s2s\ ^3S$  state.<sup>3,5</sup> Schiebel *et al.*<sup>5</sup> reported total x-ray production cross-section measurements in the

collision of two-electron  $Si^{12+}$  ions with He and suggested that electron excitation of the metastable  $^3S$  state (lifetime  $\tau = 2.8\ \mu\text{sec}$ ) is an important process. By using high-resolution x-ray spectroscopy, it is possible to use the normally troublesome metastable component to measure directly the  $1s2s \rightarrow 1s2p$  excitation cross section.

In the present work the following processes are studied using a  $F^{7+}$  beam:  $F\ 1s^2\ ^1S$  excitation to  $F\ 1s2p\ ^1P$ ,  $F\ 1s2s\ ^3S$  excitation to  $F\ 1s2p\ ^3P$ , and  $F\ 1s2s\ ^3S$  capture to  $F\ 1s2s2p\ ^4P$ . The experimental method combines high-resolution x-ray spectroscopy to identify the final atomic states, beam-foil techniques for determining the fraction of the metastable component in the primary  $F^{7+}$  beam, and standard normalization techniques for determining absolute cross sections using the total x-ray production cross sections for  $F^{9+} + He$  as a normalization.<sup>6</sup> The motivation of the present work is to measure the cross sections separately, for the first time, for the three processes mentioned above for the case of high-energy two-electron beams to compare with existing theories.<sup>7-11</sup>

### II. EXPERIMENTAL METHOD

The experiment was carried out using the Kansas State University EN tandem Van de Graaff accelerator. Beams of  $F^{3+}$  and  $F^{4+}$  ions were stripped to higher charge states by a  $10\text{-}\mu\text{g}/\text{cm}^2$  carbon poststripping foil. After stripping, single-charge-state ion beams were magnetically separated, and then focused into a target chamber approximately 10 m from the carbon stripper foil. In this arrange-

ment, 99.8% of the metastable  $1s2s\ ^3S\ F^{7+}$  [lifetime  $\tau=275\ \mu\text{sec}$  (Ref. 12)] beam produced in the stripper foil at 30 MeV will reach the target. Although formation of the  $1s2s\ ^1S$  state is also possible at the stripper foil, only 5.6% will remain at the target at 30 MeV because of the short lifetime ( $\tau=200\ \text{nsec}$ ).<sup>12</sup>

The present study is composed of two individual experiments, that is, the experiment to determine the metastable  $^3S$  state fraction in the two-electron  $F^{7+}$  ions and the high-resolution measurement of x rays induced by the collision of  $F^{7+}$  with He atoms. The metastable beam fraction was determined using a thin evaporated Ti ( $\sim 1\ \mu\text{g}/\text{cm}^2$ ) layer on a carbon foil as a target, and obtaining the TiK x rays induced by  $F^{q+}$  ion bombardment with a Si(Li) x-ray detector for the charge states  $q=4,6-8$ . It is well known that the target K x-ray production cross sections with highly ionized projectiles reflect the number of projectile K vacancies due to the target K shell to projectile K shell electron-capture process for projectiles with one or more K-shell vacancies.<sup>13</sup>

Assuming that the  $1s^2\ ^1S$  component of the  $F^{7+}$  beam produces the same number of TiK x rays as an equivalent particle beam of  $F^{q+}$  ions ( $q \leq 6$ ), and that the single K-vacancy bearing  $1s2s\ ^3S$  component of the  $F^{7+}$  beams produces the same number of TiK x rays as an equivalent particle beam of  $F^{8+}$  ions, the fraction  $f_{3S}$  of the  $1s2s\ ^3S$  component is represented as follows:

$$f_{3S} = \frac{\sigma(7+) - \sigma(6+)}{\sigma(8+) - \sigma(6+)} = \frac{Y(7+) - Y(6+)}{Y(8+) - Y(6+)}, \quad (1)$$

where  $\sigma(q+)$  and  $Y(q+)$  are TiK x-ray production cross section and x-ray yield for charge state  $q$ ,

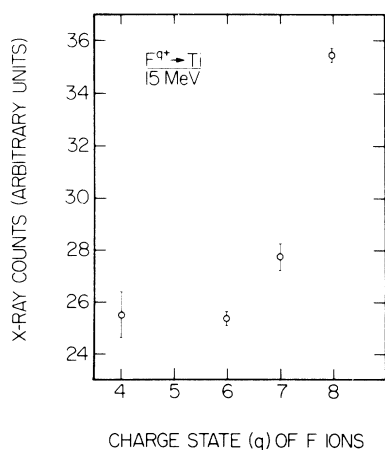


FIG. 1. TiK x-ray yields as a function of incident projectile charge state for 15-MeV F ions incident on a thin Ti target. TiK x-ray yields are normalized by the number of scattered F particles from the Ti target.

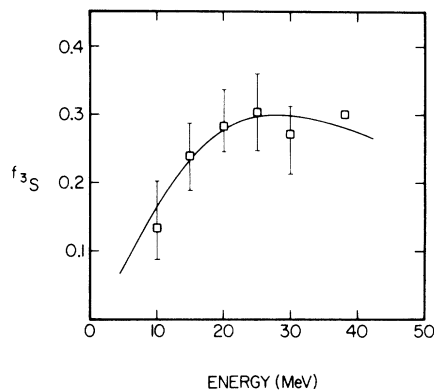


FIG. 2. Fraction of metastable  $^3S$  component ( $f_{3S}$ ) in the incident  $F^{7+}$  beam as a function of incident energy. Fractions are calculated by using Eq. (1). Solid line is drawn to guide the eye, and used in the analysis of the FK x-ray data.

respectively.

Figure 1 shows the typical TiK x-ray yield as a function of projectile charge state at the projectile energy of 15 MeV. Figure 2 shows the  $^3S$  fraction versus projectile energy obtained by measuring TiK x-ray yields for respective charge states. The fraction increases with increasing energy and appears to maximize at about 30% at energies near 25 MeV. The solid line is drawn to guide the eye, and was used for analyzing FK x-ray data.

In high-resolution measurements of FK x rays induced by collisions of  $F^{7+}$  with He, the He gas target was maintained at constant gas pressure in a differentially pumped gas cell. The pressure was monitored by a Baratron pressure gauge. The x-ray spectrometer was a 4-in. curved crystal spectrometer with a rubidium acid phthalate (RbAP) crystal which has a  $0.5 \times 12.5\ \text{mm}$  entrance slit fixed at the gas cell wall parallel to the beam. The x-ray detector was a gas-flow proportional counter with a  $2\text{-}\mu\text{m}$  Mylar window, and with a 0.5-mm slit as an image slit of the spectrometer.

The projectile beam current was measured by a Faraday cup which was set behind the gas cell, and the x-ray intensity was normalized by the integrated beam current. The gas impurities inside the gas cell were monitored by the use of a particle recoil monitor at a laboratory angle of  $35^\circ$ .

The x-ray yields were corrected for attenuation in the proportional counter window and for crystal reflectivity. Additional corrections were made to take into account the lifetime of the metastable  $^3P_1$  state [0.54 nsec (Ref. 12)] and  $^4P$  state (15 nsec for  $^4P_{5/2}$  and 2 nsec for  $^4P_{3/2,1/2}$ )<sup>12</sup> decay over the finite length of the spectrometer entrance aperture. These correction factors<sup>1</sup> are dependent on the beam velo-

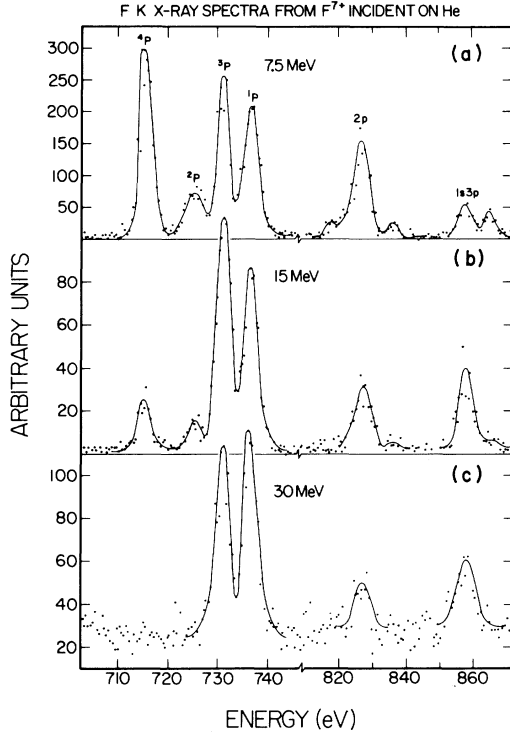


FIG. 3. FK x-ray spectra in two energy regions, 700–750 and 810–870 eV, as obtained with incident energies of 7.5, 15, and 30 MeV. Spectra include x rays due to transitions of Li-like ( $^4P$  and  $^2P$ ), He-like ( $^3P$  and  $^1P$ ), and H-like ( $2p$ ) F ions. Spectra are raw data, and are not corrected for the fraction of  $^1S$  or  $^3S$  components in the beam.

city and found to vary from 1.04 to 1.34 for the  $^3P_1$  state and from 2.73 to 5.59 for the  $^4P$  state in going from 6 to 40 MeV.

The measurement of the He gas pressure dependence of the x-ray yield revealed a linear relationship up to 80 mTorr at 15 MeV. The experimental measurements were performed at the pressure of 80 mTorr in order to minimize counting times. Single-collision conditions are assumed in this experiment based on the linear dependence of the yield on gas pressure.

In order to convert x-ray yields obtained by high-resolution measurement into x-ray production cross sections, we compared the high-resolution x-ray data for  $F^{9+}$ ,  $F^{8+}$ , and  $F^{7+}$  projectiles with the data of total x-ray production cross sections for  $F^{9+}$  given by Guffey *et al.*<sup>6</sup> and deduced absolute cross sections by using the latter for normalization.

### III. EXPERIMENTAL RESULTS

Figure 3 shows samples of x-ray spectra obtained by 7.5-, 15-, and 30-MeV  $F^{7+}$  ions incident on He. In the low-energy region between 710 and 740 eV, x-ray peaks due to transitions from Li-like  $1s2s2p^4P$  and  $1s2s2p^2P$  states and He-like  $1s2p^3P$  and  $1s2p^1P$  states to the corresponding ground states are resolved. At energies above 820 eV, x rays due to  $2p \rightarrow 1s$  and  $1s3p \rightarrow 1s^2$  transitions are observed. The other x rays resulting from the transitions of excited He-like and H-like ions are also observed with less intensity at energies above 870 eV, though they are not shown in the figure. Table I summarizes the calculated and measured transition energies for two- and three-electron ions of F. The calculated fluorescence yields<sup>12</sup> are also given for reference.

Prior to discussing the formation of each of the

TABLE I. Two- and three-electron x-ray transition energies and fluorescence yields of F.

Transition	Calculated energy (eV) <sup>a</sup>	$\omega_K$ <sup>a</sup>	Measured energy (eV) <sup>b</sup>
$1s2p^2^2S \rightarrow 1s^22p^2P$	697.8	0.14	
$1s2s2p^4P \rightarrow 1s^22s^2S$	714.7	0.18	714.8
$1s2p^2^4P \rightarrow 1s^22p^2P$	717.0	0.02	
$1s2s2p^2P_- \rightarrow 1s^22s^2S$	725.0	0.31	
$1s2p^2^2P \rightarrow 1s^22p^2P$	725.0	0.99	725.3
$1s2p^2^2D \rightarrow 1s^22p^2P$	723.0	0.02	
$1s2p^3P \rightarrow 1s^2^1S$	730.7	0.32	
$1s2s2p^2P_+ \rightarrow 1s^22s^2S$	730.8	0.01	731.0
$1s2p^1P \rightarrow 1s^2^1S$	735.6	1.00	737.7

<sup>a</sup>Taken from Ref. 12.

<sup>b</sup>The error in these measurements is  $\sim \pm 1$  eV.

initial states leading to the x rays listed in Table I and shown in Fig. 3, a general discussion concerning the formation of the two- and three-electron configurations of F from the  $F^{7+} 1s^2 1S$  ground state and the  $F^{7+} 1s 2s^3 S$  metastable beam component in collisions with He is informative.

The K x-ray emitting *three-electron configurations* of F formed with  $n=1$  and 2 electrons are the  $1s 2s 2p$  and  $1s 2p^2$  configurations. The  $1s 2s 2p$  configuration can be formed from the  $1s 2s^3 S$  beam component by direct electron capture to the vacant  $2p$  level, or it can be formed from the  $1s^2 1S$  beam component by a two-electron process consisting of either direct capture to the vacant  $2p$  level simultaneous with  $1s \rightarrow 2s$  excitation or direct capture to the vacant  $2s$  level simultaneous with  $1s \rightarrow 2p$  excitation. The  $1s 2p^2$  configuration can be formed from the  $1s^2 1S$  beam component by a two-electron process consisting of direct capture to the vacant  $2p$  level simultaneous with  $1s \rightarrow 2p$  excitation. It can also be formed from the  $1s 2s^3 S$  beam component by a two-electron process consisting of direct capture to the vacant  $2p$  level simultaneous with  $2s \rightarrow 2p$  excitation. The one-electron process is expected to be dominant over the two-electron processes proposed here.

The K x-ray emitting *two-electron configuration* of F formed with  $n=1$  and 2 electrons is the  $1s 2p$  configuration. This configuration can be formed from the  $1s^2 1S$  ground state by  $1s \rightarrow 2p$  electron excitation. For pure Coulomb excitation only the  $1s 2p^1 P$  final state is allowed. The  $1s 2p$  configuration can also be formed from the  $1s 2s^3 S$  beam component by  $2s \rightarrow 2p$  electron excitation. For pure Coulomb excitation only the  $1s 2p^3 P$  final state is allowed. These arguments suggest that the  $^1 P$  and  $^3 P$  formation cross sections reflect the  $1s \rightarrow 2p$  and  $2s \rightarrow 2p$  electron-excitation cross sections, respectively.

We now turn to the discussion of the excitation of the FK x rays in the order of increasing x-ray energy.

The lowest-energy x ray from the configurations discussed above is the  $1s 2p^2 2S \rightarrow 1s^2 2p^2 P$  transition calculated to be at 697.8 eV. No observable x ray is seen at this energy which is consistent with the facts that the state would be formed by a two-electron process and that the state has a low fluorescence yield.

The x ray observed at 714.8 eV is attributed to the  $1s 2s 2p^4 P \rightarrow 1s^2 2s^2 S$  transition which can be induced by direct electron capture to the  $2p$  level for incident  $1s 2s^3 S$  metastable states. Little contribution is expected from the  $1s 2p^2 4P \rightarrow 1s^2 2p^2 P$  transition which requires a two-electron process and which has a very low fluorescence yield. The x-ray transitions from the  $^4 P$  states give the most intense

contribution to the x-ray spectrum at low projectile energies. The x-ray intensity associated with the decay of the  $^4 P$  states decreases with increasing projectile energy and becomes lost in the x-ray background above incident energies of 30 MeV.

The x ray observed at 725.3 eV is attributed to three possible transitions which are not resolved with the present energy resolution. The  $1s 2s 2p^2 P_- \rightarrow 1s^2 2s^2 S$  transition is induced by capture to the metastable  $^3 S$  ion, whereas the  $1s 2p^2 2P$ ,  $^2 D$  states require two-electron processes. The 725.3-eV transition decreases with increasing beam energy similar to that observed for the  $^4 P$  states which supports a capture formation mechanism.

The x ray observed at 731.0 eV is attributed to the  $1s 2p^3 P \rightarrow 1s^2 1S$  transition which is induced by  $2s$ - $2p$  electron excitation of the  $1s 2s^3 S$  metastable beam component. The close-lying  $1s 2s 2p^2 P_+ \rightarrow 1s^2 2s^2 S$  transition which is induced by  $2p$  capture to the  $1s 2s^3 S$  state cannot be resolved from the  $1s 2p^3 P \rightarrow 1s^2 1S$  transition. The  $1s 2s 2p^2 P_+$  state has a very low fluorescence yield and is thus not expected to contribute significantly to the 731.0-eV x ray.

The x ray observed at 737.7 eV is attributed to the  $1s 2p^1 P \rightarrow 1s^2 1S$  transition which is induced by  $1s \rightarrow 2p$  electron excitation of the  $1s^2 1S$  state. No close-lying transitions interfere with this transition. It should be noted that the formation of the  $1s 2p^1 P$  state from the  $1s 2s^3 S$  state requires a spin flip as does formation of the  $1s 2p^3 P$  state from the  $1s^2 1S$  state. Such spin-flip contributions to the electron-excitation process are assumed to be negligible in these considerations.

The higher-lying transitions above 820 eV are attributed primarily to the  $np \rightarrow 1s$  hydrogenlike transitions and the  $1snp \rightarrow 1s^2 (n > 2)$  heliumlike transitions. Two of these transitions are indicated in Fig. 3 by the initial-state configuration. The hydrogenlike transitions are formed by ionization plus electron excitation of either the  $1s^2 1S$  or  $1s 2s^3 S$  components. The heliumlike transitions are formed by  $1s \rightarrow np$  excitation of the  $1s^2 1S$  beam component or by  $2s \rightarrow np$  excitation of the  $1s 2s^3 S$  beam component.

Figure 4 shows the measured cross sections for electron capture ( $1s 2s^3 S \rightarrow 1s 2s 2p^4 P$ ) and electron excitation ( $1s 2s^3 S \rightarrow 1s 2p^3 P$  and  $1s^2 1S \rightarrow 1s 2p^1 P$ ) as a function of projectile energy. These data points were obtained from the measured x-ray yields, the measured metastable fractions shown in Fig. 2, and the fluorescence yields given in Table I. Cross sections for electron capture leading to the formation of the  $^2 P$  and  $^2 P_-$  states and for ionization leading to the H-like  $2p$  state cannot be directly analyzed because the contributions of the  $^1 S$  or  $^3 S$  beam com-

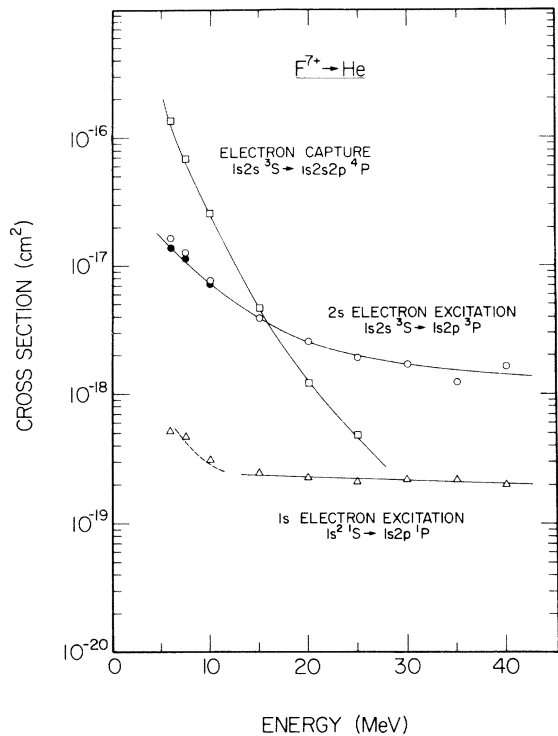


FIG. 4. Cross sections of electron capture and 2s electron excitation of  ${}^3S$   $F^{7+}$  ions, and 1s electron excitation of  ${}^1S$   $F^{7+}$  ions as a function of incident projectile energy. Cross sections are corrected for the fraction of  ${}^1S$  or  ${}^3S$  components. Solid circles are the data which are obtained by subtracting  ${}^2P_+$  capture cross sections from the measured total cross sections shown by open circles. Solid lines are drawn to guide the eye.

ponents cannot be separated.

It is found that the electron-capture process dominates in the collision of metastable  $1s2s$   ${}^3S$   $F^{7+}$  ions with He at low projectile energy. The electron capture, however, decreases steeply with increasing energy, similar to that observed for electron capture by bare  $F^{9+}$  or one-electron  $F^{8+}$  ions incident on He. The cross section for 2s electron excitation decreases with increasing projectile energy. The solid circles are measurements of 2s-2p electron excitation which were obtained by subtracting from the total cross sections the contributions from 2p electron capture associated with the formation of the  ${}^2P_+$  state from the initial  ${}^3S$  configuration. The contributions from the  ${}^2P_+$  state were calculated based on the measured capture cross section data for transitions from the  ${}^4P$  state. We assumed that the 2p capture cross section ( ${}^3S + 2p \rightarrow {}^2P_+$ ) should be the same as the cross section for  ${}^3S + 2p \rightarrow {}^4P$ . A theoretical fluorescence yield of  $\omega = 0.01$  for  ${}^2P_+$  to ground-state transitions<sup>12</sup> was used in the calculation. The calculated  ${}^2P_+$  cross sections are  $2.2 \times 10^{-18}$  cm<sup>2</sup> at 6 MeV,

$1.1 \times 10^{-18}$  cm<sup>2</sup> at 7.5 MeV, and  $4.0 \times 10^{-19}$  cm<sup>2</sup> at 10 MeV and fall off steeply at higher energies. In general, the contribution is found to be relatively low. The measured 2s-2p electron excitation as a function of projectile energy shows a relationship close to a  $1/E$  dependence. It is noted that, at high energies, the excitation process prevails over the capture process in the collision of the  ${}^3S$  projectile state with He.

The measured cross sections for 1s electron excitation of the  ${}^1S$  state are nearly constant over the energy range of the present work. Further, excitation of  ${}^3S$  to  ${}^3P$  is more probable than the excitation of  ${}^1S$  to  ${}^1P$ . Below 15 MeV there is a rise in the  $1s \rightarrow 2p$  excitation peak due to the double collisions (see dashed region of  $1s^2$   ${}^1S \rightarrow 1s2p$   ${}^1P$  curve in Fig. 4). This rise is due to an  $\sim 1\%$  fraction of one-electron beam formed near the collision region leading to the  $1s \rightarrow 1s2p$   ${}^1P$  capture process which has a cross section one to two orders of magnitude greater than the  $1s^2$   ${}^1S \rightarrow 1s2p$   ${}^1P$  excitation cross section below 15 MeV.

#### IV. DISCUSSION

In the collision of metastable  $F^{7+}$  ions, the most prominent process is electron capture. The capture cross sections are one order of magnitude larger than any other process at low energies. Although there are several models<sup>7-9</sup> to predict the electron-capture process by bare ions, no present theoretical predictions apply for the electron capture by heavy ions which have one or more electrons initially. It is

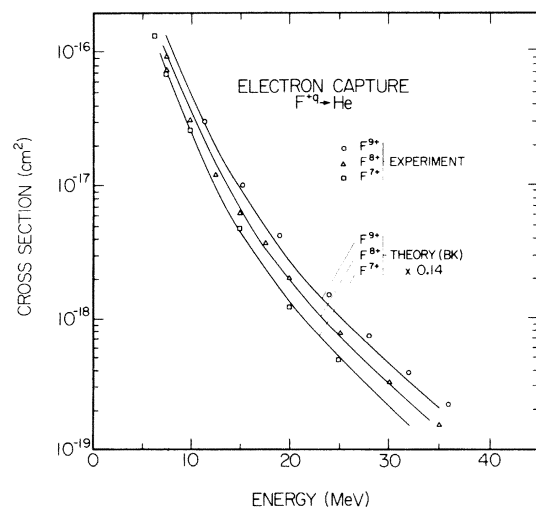


FIG. 5. Electron-capture cross sections for  $F^{7+}$ ,  $F^{8+}$ , and  $F^{9+}$  ions incident on He, as a function of incident energy. Experimental  $F^{8+}$  and  $F^{9+}$  data are taken from Refs. 2 and 6, respectively. Theoretical cross sections are obtained from the BK calculations multiplied by 0.14.

well known that the Oppenheimer-Brinkman-Kramers (OBK) approximation overestimates the magnitude of the capture cross sections.<sup>6-9</sup> Guffey *et al.*<sup>6</sup> measured total x-ray yields due to electron capture of fully ionized ions of F, O, N, and C on He, and found that a scaled OBK calculation agreed with the experimental energy and atomic-number dependence of the electron-capture cross sections.

In the present study, we discuss the charge-state dependence of the electron-capture cross sections in terms of the scaled OBK theory. Figure 5 shows the measured  $F^{7+}$  electron-capture cross sections, together with the experimental data on  $F^{8+}$  and  $F^{9+}$  capture and scaled OBK calculations<sup>6</sup> for each incident charge. The data for  $F^{9+}$  ions were given by Guffey *et al.*<sup>6</sup> The capture cross sections for  $F^{8+}$  ions were obtained from the x-ray production cross-section data given by Tawara *et al.*,<sup>2</sup> using  $\omega=0.49$  as the fluorescence yield.<sup>12</sup> The theoretical capture cross-section calculations were obtained using a scaling factor of 0.14 in the OBK calculations. It is found that the measured electron-capture cross sections decrease systematically with decrease of the incident ion charge states, and that the scaled OBK calculations agree with the experimental results.

As mentioned above, Schiebel *et al.*<sup>5</sup> deduced the  $2s-2p$  electron-excitation cross section from the total x-ray yield data in  $Si^{12+}$ -He collisions. Recently, McGuire *et al.*<sup>10</sup> calculated  $2s-2p$  excitation probability as a function of impact parameter  $b$  for proton projectiles based on time-dependent perturbation theory, referred to as the semiclassical Coulomb approximation (SCA). They found a different

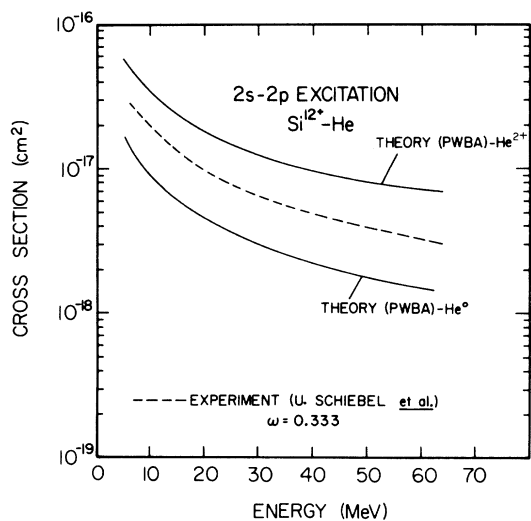


FIG. 6. Comparison between measured and calculated  $2s-2p$  excitation cross sections in  $Si^{12+}$ -He collisions as a function of incident projectile energy. Data are from Ref. 5 and theory from Ref. 11.

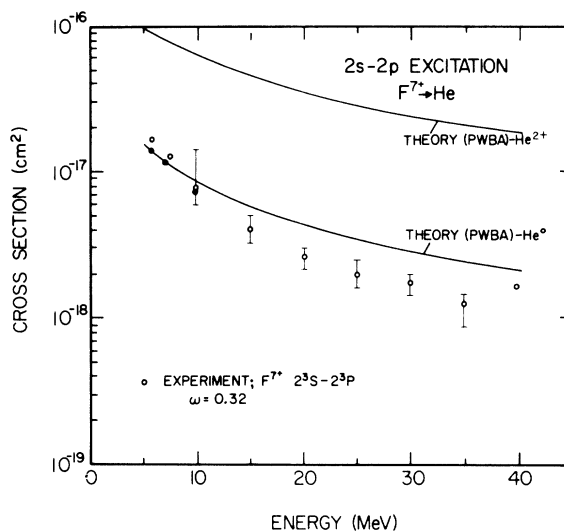


FIG. 7. Comparison between measured and calculated  $2s-2p$  excitation cross sections in  $F^{7+}$ -He collisions as a function of incident projectile energy. Solid circles are the  $2s$  excitation cross sections with the contribution of  ${}^2P_+$  capture subtracted. Theoretical cross sections of  $He^0 + F^{7+}$  and  $He^{2+} + F^{7+}$  are taken from McGuire and Simony (Ref. 11).

target-atomic-number behavior for intrashell excitation ( $2s-2p$ ) than one obtains for intershell excitation ( $1s-2p$ ). More recently, McGuire and Simony<sup>11</sup> extended these calculations to include systems where the projectile contains electrons in order to compare with the  $Si^{12+} + He$  data of Schiebel *et al.* and the present results for  $F^{7+} + He$ . They derive and evaluate plane-wave Born-approximation (PWBA) cross sections for  $2s-2p$  excitation by  $He^{2+}$  and  $He^0$  projectiles. Figure 6 shows the  $2s$  electron-excitation cross section deduced from the total cross sections for  $Si^{12+} + He$  by Schiebel *et al.*<sup>5</sup> using a fluorescence yield of 0.333 calculated by Tunnell *et al.*<sup>12</sup> together with the calculations of McGuire and Simony.<sup>11</sup> Figure 7 shows the measured  $2s$  electron-excitation cross sections for metastable  ${}^3S$  ions of the two-electron  $F^{7+}$  beam, together with the PWBA calculations<sup>11</sup> of the cross section.

In the PWBA calculation for the  $2s$  excitation by  $He^{2+}$  ions incident on the  $1s2s\ {}^3S$  metastable ions, it was assumed that the target atomic charge was  $Z-1$  since the  $n=2$  electron is well outside the  $n=1$  electron. The electron in the  $n=2$  level is treated as hydrogenic and the  $2s-2p$  energy separations are taken as 12.9 eV for Si and 8.6 eV for  $F^{7+}$ . The  $He^{2+}$  predictions fall a factor of 2 above the data for  $Si^{12+}$  and one order of magnitude above the data for  $F^{7+}$ . In the PWBA calculation for  $2s$  excitation by  $He^0$  ions incident on the  $1s2s\ {}^3S$  ions, the same assumptions were made regarding the  $Si^{12+}$

and  $F^{7+}$  ions, however, the PWBA expression for the effective  $He^0$  charge as a function of momentum transfer was used. These results compare more favorably with the data for  $F^{7+}$  (see Fig. 7) and underestimate the data by a factor of 2 for  $Si^{12+}$  (see Fig. 6). These comparisons of the calculations to data for  $Si^{12+}$  and  $F^{7+}$  on He indicate that the He electrons play a significant role in the  $2s$ - $2p$  intrashell excitation of  $F^{7+}$ . Unfortunately, the PWBA theory of McGuire and Simony for  $He^0 + F^{7+}$  and  $He^0 + Si^{12+}$  does not give a consistent picture. There could be some difficulty with the total cross-section subtraction technique of Schiebel *et al.* used to obtain the Si results. On the other hand, atomic distortion effects on the orbitals of  $F^{7+}$  during the collision could also be playing a role in the excitation process and are not included in the calculations of McGuire and Simony. It is known that ionization cross sections of H atoms in  $H^0$ -H collisions are smaller than that in  $H^+$ -H collisions.<sup>14</sup> There is also experimental evidence showing discrepancy of ionization cross sections of He between  $He^{2+}$ -He and  $He^0$ -He collisions.<sup>15</sup>

The  $1s$  electron excitation for one-electron  $1s$   $F^{8+}$  ions and three-electron  $1s^2 2s$   $F^{6+}$  ions incident on He were previously investigated by high-resolution x-ray measurements. The measured excitation cross sections were shown to agree well with PWBA theory if one assumes, in the theoretical calculation, that the  $1s$  electrons of He do not have any screening effect on the He nucleus.

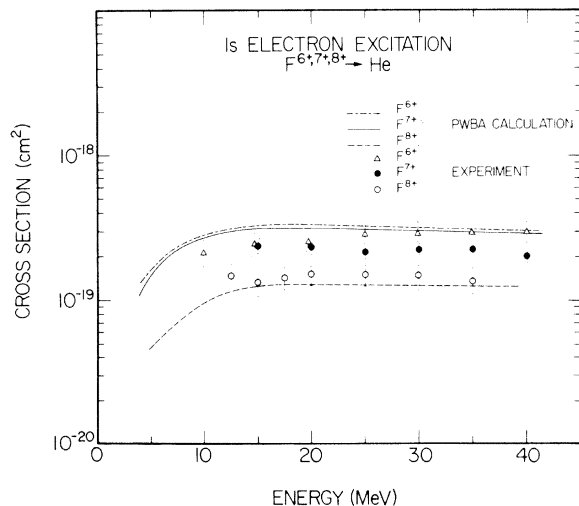


FIG. 8. Measured and calculated  $1s$  electron-excitation cross sections in  $F^{6+}$ -,  $F^{7+}$ -, and  $F^{8+}$ -He collisions as functions of incident projectile energy. Theoretical cross sections are obtained by a PWBA calculation assuming that screening of the  $1s$  orbital electrons of He are neglected.

Figure 8 shows the measured  $1s$  excitation cross sections for two-electron  $1s^2$   $F^{7+}$  ions incident on He, together with the measured  $1s$  excitation cross sections for  $F^{6+}$  and  $F^{8+}$  ions and the theoretical calculations based on the PWBA with no screening. The  $F^{7+}$  cross sections lie between the  $F^{6+}$  and the  $F^{8+}$  data, and all three of the cross sections show a similar flat energy dependence. In the theoretical calculation, experimentally obtained transition energies between  $1s$  and  $nl$  levels are used. The PWBA theory is found to agree with the measured data. It is noted that the  $F^{6+}$  cross sections are almost the same magnitude as the  $F^{7+}$  cross sections in the PWBA theory, whereas the experimental data show some differences. The main difference between the  $F^{6+}$  ( $F^{7+}$ ) and  $F^{8+}$  excitation cross sections is a statistical factor of 2 pertaining to the number of  $K$ -shell electrons. The measured cross sections at energies lower than 10 MeV are not shown in the figure because the data are considered to include some contribution from double collisions of the incident ions in the target gas as discussed previously.

## V. CONCLUSIONS

$K$  x-ray production cross sections are measured for high-velocity two-electron ions incident on helium. It is demonstrated that three separate processes are primarily responsible for the total  $K$  x-ray production cross section as suggested by Schiebel *et al.*<sup>5</sup> This is done by resolving the final states formed in the collision. Two of the processes occur through the long-lived metastable  $1s 2s^3 S$  component of the beam and the third occurs through the ground-state  $1s^2 1S$  component of the beam. It is expected that these three processes are active in all two-electron beam experiments unless extreme care is taken in forming the ion beam in a pure state.

Having identified the x-ray features corresponding to  $2s \rightarrow 2p$  excitation,  $nl$  capture, and  $1s \rightarrow 2p$  excitation, the cross sections were deduced and compared to theory. The  $2s \rightarrow 2p$  excitation cross section is observed to fall off with energy since the target-projectile relative velocity is well above the  $2s$  orbital velocity. The data agree with a Born-approximation calculation for  $F^{7+} + He^0$ . The  $F^{7+}$  capture cross section has the same velocity dependence as the  $F^{8+}$  and  $F^{9+}$  measurements,<sup>2,6</sup> and a magnitude that is consistent with a charge state scaling from either  $F^{8+}$  or  $F^{9+}$ . The  $1s \rightarrow 2p$  excitation cross section is observed to be rather flat since the target-projectile relative velocity is near the  $1s$  orbital velocity. The magnitude of this cross section agrees fairly well with Born-approximation calcula-

tions and with the measured  $F^{6+}$  excitation cross section.<sup>4</sup>

Based on the agreement between theory and the present experiment, the  $1s$  electrons of He screen the He nucleus for  $2s \rightarrow 2p$  excitation of  $F^{7+} 1s 2s$  ions and does not screen the He nucleus for  $1s \rightarrow 2p$  excitation of  $F^{7+} 1s^2$  ions. This same argument could not be made for the  $Si^{12+}$  data of Schiebel *et al.*<sup>5</sup>

A final note to be made is that the delicate task of assigning the observed x-ray transitions to the three processes discussed above was evidently properly executed. The assignments are corroborated by the agreement between existing theory and by the com-

parisons with data in which the excitation processes are clearly defined.

#### ACKNOWLEDGMENTS

The authors would like to thank Professor J. M. McGuire for valuable discussions, and Professor C. P. Bhalla, T. W. Tunnell, and C. Can for providing the theoretical calculation of fluorescence yields and lifetimes of excited heavy ions. This work was performed with support from the Division of Chemical Sciences, U.S. Department of Energy.

\*Present address: Toshiba Research & Development Center, Kawasaki, Japan.

<sup>1</sup>F. F. Hopkins, R. L. Kauffman, C. W. Woods, and Patrick Richard, *Phys. Rev. A* **9**, 2413 (1974).

<sup>2</sup>H. Tawara, Patrick Richard, K. A. Jamison, and Tom J. Gray, *J. Phys. B* **11**, L615 (1978).

<sup>3</sup>H. Tawara, Patrick Richard, K. A. Jamison, Tom J. Gray, J. Newcomb, and C. Schmiedekamp, *Phys. Rev. A* **19**, 1960 (1979).

<sup>4</sup>H. Tawara, M. Terasawa, Patrick Richard, Tom J. Gray, P. Pepmiller, J. Hall, and J. Newcomb, *Phys. Rev. A* **20**, 2340 (1979).

<sup>5</sup>U. Schiebel, B. L. Doyle, J. R. Macdonald, and L. D. Ellsworth, *Phys. Rev. A* **16**, 1089 (1977).

<sup>6</sup>J. A. Guffey, L. D. Ellsworth, and J. R. Macdonald, *Phys. Rev. A* **15**, 1863 (1977).

<sup>7</sup>H. C. Brinkman and H. A. Kramers, *Proc. Acad. Sci. (Amsterdam)* **33**, 973 (1930); J. R. Oppenheimer, *Phys. Rev.* **31**, 369 (1928).

<sup>8</sup>V. S. Nikolaev, *Zh. Eksp. Teor. Fiz.* **51**, 1263 (1966)

[*Sov. Phys.—JETP* **24**, 847 (1967)].

<sup>9</sup>Grzegorz Lapicki and William Losonsky, *Phys. Rev. A* **15**, 890 (1977).

<sup>10</sup>J. M. McGuire, D. L. Land, J. G. Brennan, and G. Basbas, *Phys. Rev. A* **19**, 2180 (1979).

<sup>11</sup>J. H. McGuire and P. R. Simony, *Phys. Rev. A* **22**, 2270 (1980).

<sup>12</sup>T. W. Tunnell, C. Can, and C. P. Bhalla, *IEEE Trans. Nucl. Sci.* **NS-26**, 1124 (1979).

<sup>13</sup>For gas targets, see J. R. Macdonald, L. Winters, M. D. Brown, T. Chiao, and L. D. Ellsworth, *Phys. Rev. Lett.* **29**, 1291 (1972). For solid targets, see R. K. Gardner, Tom J. Gray, Patrick Richard, Carl Schmiedekamp, K. A. Jamison, and J. M. Hall, *Phys. Rev. A* **19**, 1896 (1979).

<sup>14</sup>D. R. Bates and G. W. Griffing, *Proc. Phys. Soc. London, Sect. A* **66**, 961 (1953).

<sup>15</sup>L. J. Puckett, G. O. Taylor, and G. W. Martin, *Phys. Rev.* **178**, 271 (1969).